Time- and Frequency-Synchronization for Spatially Interpolated OFDM

Peter Klenner, Karl-Dirk Kammeyer
Dept. of Communications Engineering
University of Bremen, 28359 Bremen, Germany
Email: klenner@ant.uni-bremen.de

Sandra Knörzer, Werner Wiesbeck
IHE, University of Karlsruhe
76131 Karlsruhe, Germany
Email: Sandra.Knoerzer@ihe.uka.de

***Abstract*— OFDM is commonly known as a low-complexity scheme to cope with frequency-selective channels. However, a major obstacle for reliable data-transmission is constituted by rapidly fading channels. This is due to fast fading leading to a loss of orthogonality among neighboring subcarriers giving rise to intercarrier interference. A possible approach to alleviate channel estimation is the use of a linear antenna array at the receiver, which allows for computing virtual non-moving antennas by linearly combining the antenna signals. Timing synchronisation is crucial in this setting. A correct timing basis is required to have the output of the linear combination lead to an effectively time-invariant channel. A novel, robust timing approach is presented which takes into account all antenna signals and which exploits the cyclic prefix' redundancy without introducing additional training overhead. That same approach is also shown to be applicable with advantage to estimate receiver-side frequency offsets.**

I. Introduction

To cope with the channel's rapid fluctuations the authors of [1] proposed to apply a uniform linear antenna array (ULA) at the receiver side. By means of interpolation this ULA serves for creating virtual antennas which are seemingly non-moving. Thereby, the effective channel becomes time-invariant and intercarrier interference is avoided. In [1] the chosen transmission scheme, i.e., differential PSK, allowed for noncoherent reception. In [2] channel estimation approaches were described and shown to be superior in BER performance.

For the spatial interpolation (SI) scheme to work, reliable synchronization is indispensable. We will therefore contribute a time- and frequency synchronization scheme for continuous transmission which exploits the inherent correlation of the cyclic prefix (CP). Assuming burst transmission this approach is well known [3], [4], [5]. Although it has been designed for AWGN transmission, it can be utilized for multipath influence, too, if the correlation is extended only over the part of the CP which is unconsumed by the channel impulse response. In this case the correlation output will establish a flat region which leads to considerable variance in the detected start of the FFT-window. Thus, the correlation technique is deemed flawed and other techniques applying specific pilot sequences with good correlation properties are preferred [5].

Of course, these sequences lower the achievable data-rate. Instead, we take a new look at the correlation technique and present two measures to improve it. These measures are derived from a maximum-likelihood approach which jointly considers all antenna signals and bases the positioning of the FFT-window as well as the frequency offset estimate not only on one OFDM symbol but on several OFDM symbols. These measures overcome the drawback of the flat region and render the correlation technique into a reliable FFT-window positioning technique even for fast fading channels.

In order to substantiate the effectiveness of the interpolation scheme combined with synchronization we provide simulation results for statistical channels (WSSUS) as well as for realistic channel models which are obtained from ray-tracing. Here, we consider the scenario of a high-speed train which is equipped with an ULA.

II. System Model

Our system model ist depicted in Fig. 1. Binary data $b(\xi) \in \{0,1\}$ are convolutionally encoded (CC) and randomly bit-interleaved. After mapping the coded bits to a QPSK signal constellation differential modulation is performed in time direction yielding transmit symbols $d_\nu(i)$ at the ν-th subcarrier in the i-th OFDM-symbol. We define the number of subcarriers to be N, and the length of the CP to be N_g, and $Z = N + N_\mathrm{g}$. After IFFT and CP-insertion the OFDM-transmit signal in complex equivalent baseband notation reads

$$x(k) = \frac{1}{\sqrt{N}} \sum_{i=-\infty}^{\infty} \sum_{\nu=0}^{N-1} d_\nu(i) \mathrm{e}^{\mathrm{j}2\pi\nu(k-iZ)/N} g(k-iZ) \tag{1}$$

with the rectangular filter function $g(k) = 1$ for $-N_\mathrm{g} \leq k \leq N-1$, and 0 otherwise. The signal is received over the time-variant channel $h_{\ell,a}(k)$ at the a-th antenna with tap delay index ℓ and time instant k. It is assumed that the length of the channel impulse response, L, does not exceed the CP. The received signal reads

$$y_a(k) = \mathrm{e}^{\mathrm{j}2\pi\varepsilon k/N} \sum_{\ell=0}^{L-1} h_{\ell,a}(k) x(k-\ell-\theta) + n_a(k)\,, \tag{2}$$

where $n_a(k)$ denotes additive white Gaussian noise with variance σ_n^2, θ the unknown but deterministic arrival time, and ε a frequency offset normalized to the subcarrier spacing. Subsequently, it is our intent to estimate θ as

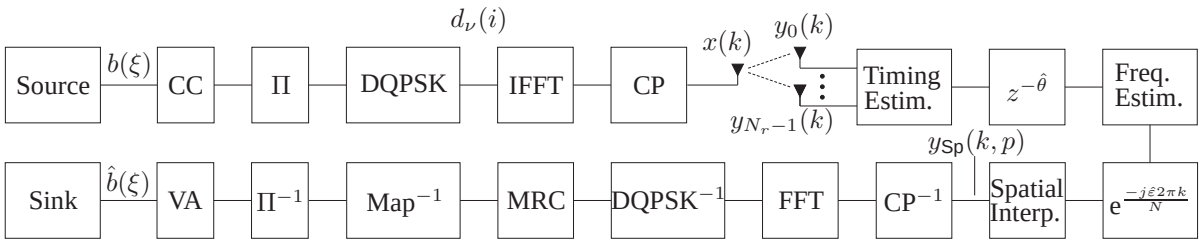

Fig. 1. OFDM-Transceiver with spatial interpolation, time and frequency synchronisation

well as ε. In Sec. III we detail a two-stage approach which determines in a first step the timing offset and secondly the freequency offset.

For the SI to work a linear antenna array is required which is composed of closely spaced antennas. Thus, the antennas will receive the transmit signal through impulse responses which are delayed replica of each other. The delay D depends on the antenna spacing and the mobile's speed. Thus, Eq. (2) is equivalent to

$$y_a(k) = \mathrm{e}^{\frac{\mathrm{j}2\pi\varepsilon k}{N}} \sum_{\ell=0}^{L-1} h_\ell(k-aD)x(k-\ell-\theta)+n_a(k)\,. \quad (3)$$

The central assumption here is that $h_{\ell,a}(k) = h_\ell(k-aD)$, which is violated in practice by mutual antenna coupling. The influence of the latter will be shown in the simulation results on the basis of ray-tracing simulation data. To describe the SI approach in more detail we assume ideally delayed impulse responses.

Beforehand the received samples of all antennas for the k-th time instant are collected in the vector $\boldsymbol{y}(k)$ defined by

$$\boldsymbol{y}(k) = [y_0(k), \cdots, y_{N_r-1}(k)]^{\mathrm{T}}\,. \quad (4)$$

The time and frequency compensated vector then reads

$$\tilde{\boldsymbol{y}}(k) = \mathrm{e}^{-\mathrm{j}2\pi\hat{\varepsilon}k/N}\boldsymbol{y}(k+\hat{\theta})\,. \quad (5)$$

The idea is now to implement a Wiener filter which at its output delivers an OFDM signal which has been received through a time-invariant channel, $h_\ell(P)$, at an arbitrary time instant P (cf. [1]). Hence, after removing frequency offset and timing offset we wish to generate the signal

$$f(k) = \sum_{\ell=0}^{L-1} h_\ell(P)x(k-\ell)\,. \quad (6)$$

This is achieved by linearly combining the received antenna signals, which are already time and frequency compensated, i.e.,

$$y_{\mathsf{Sp}}(k,p) = \mathbf{w}^{\mathrm{H}}(k,p)\tilde{\boldsymbol{y}}(k)\,. \quad (7)$$

The Wiener filter output is denoted by $y_{\mathsf{Sp}}(k,p)$. Its coefficients are found by solving $\mathbf{w}(k,p) = \mathrm{argmin}_{\tilde{\mathbf{w}}}\,\mathrm{E}\{|f(k)-\tilde{\mathbf{w}}^{\mathrm{H}}\tilde{\boldsymbol{y}}(k)|^2\}$ which yields the Wiener-Hopf equation. One can choose to generate several virtual antennas, i.e. $p > 1$, for a given number of N_r receive antennas. Extensive simulations indicate that it is advantageous to compute a virtual antenna for each actual antenna. The origins of these virtual antennas are the starting positions of the original antennas.

The virtual antenna signals are subsequently passed through the FFT after the CP-removal. Upon differential demodulation maximum ratio combining (MRC) takes place followed by a demapping to recover the coded bits which are deinterleaved and decoded by the Viterbi algorithm (VA).

III. Timing Synchronization

We describe now our novel method to determine estimates for the timing and frequency offset, $\hat{\theta}$ and $\hat{\varepsilon}$, respectively. All received symbols for the i-th OFDM symbol are assembled in the vector

$$\boldsymbol{z}_\theta(i) = [\boldsymbol{y}(iZ-N_{\mathrm{g}}+\theta), \cdots, \boldsymbol{y}(iZ+N-1+\theta)]^{\mathrm{T}}\,. \quad (8)$$

To find the arrival time θ we take into account all OFDM-symbols as well as all antenna signals. Hence, we want to maximize the log-likelihood function

$$\lambda(\theta,\varepsilon) = \log p\big(\theta,\varepsilon|\ \boldsymbol{z}_\theta(-\infty), \cdots, \boldsymbol{z}_\theta(\infty)\ \big)\,, \quad (9)$$

where we have introduced the probability density $p\big(\theta,\varepsilon|\boldsymbol{z}_\theta(-\infty), \cdots, \boldsymbol{z}_\theta(\infty)\big)$ for timing and frequency offset conditioned on all OFDM-symbols. This is equivalent to maximizing the log-likelihood function, $\lambda_0(\theta,\varepsilon)$, for θ and ε given by

$$\lambda_0(\theta,\varepsilon) = \sum_{i=-\infty}^{\infty} \log p\big(\boldsymbol{z}_\theta(i)|\theta,\varepsilon\big)\,. \quad (10)$$

The partial log-likelihood function $p(\boldsymbol{z}_\theta(i)|\theta,\varepsilon)$ is proportional to (cf. [3])

$$\log p(\boldsymbol{z}_\theta(i)|\theta,\varepsilon) \propto \sum_{\mu=-N_s-\theta+iZ}^{-1-\theta+iZ} \log \frac{p(\boldsymbol{y}(\mu),\boldsymbol{y}(\mu+N))}{p(\boldsymbol{y}(\mu))p(\boldsymbol{y}(\mu+N))}\,. \quad (11)$$

Note the introduction of the variable N_s in (11). It determines the number of symbols within the CP which are correlated. It is an important parameter when multipath channels are involved, since then a part of the CP is impaired by ISI. Adjusting N_s serves for excluding those portions of the CP from the sum.

If the number of subcarriers is large, the central limit theorem allows for the assumption that the OFDM-signal (1) is Gaussian. Hence, the received signal (3) is Gaussian as well. With the definition of $\boldsymbol{y}_k = [\boldsymbol{y}^{\mathrm{T}}(k), \boldsymbol{y}^{\mathrm{T}}(k+N)]^{\mathrm{T}}$ we have therefore

$$\log p(\boldsymbol{z}(i)|\theta,\varepsilon) \propto \sum_{\mu=-N_s+\theta+iZ}^{-1+\theta+iZ} -\boldsymbol{y}_\mu^{\mathrm{H}}\mathbf{C}_0^{-1}\boldsymbol{y}_\mu + \boldsymbol{y}^{\mathrm{H}}(\mu)\mathbf{C}_1^{-1}\boldsymbol{y}(\mu) + \boldsymbol{y}^{\mathrm{H}}(\mu+N)\mathbf{C}_1^{-1}\boldsymbol{y}(\mu+N)\,. \quad (12)$$

The correlation matrices are given by $\mathbf{C}_0 = \mathrm{E}\{\boldsymbol{y}_k^{\mathrm{H}}\boldsymbol{y}_k\}$ and $\mathbf{C}_1 = \mathrm{E}\{\boldsymbol{y}(k)^{\mathrm{H}}\boldsymbol{y}(k)\} = \mathrm{E}\{\boldsymbol{y}(k+N)^{\mathrm{H}}\boldsymbol{y}(k+N)\}$. The underlying autocorrelation function is given by

$$r_{yy}(a-a',k-k') = \mathrm{E}\{y_a(k)y_{a'}^*(k')|\theta,\varepsilon\} \qquad (13)$$
$$= \sigma_x^2 \mathrm{e}^{\frac{\mathrm{j}2\pi\varepsilon(k-k')}{N}}\Theta((a-a')D)\delta_{(k-k')_N} + \sigma_n^2\delta_{a-a',k-k'}$$

with the power σ_x^2 of the transmit signal (1), the time-correlation function $\Theta(\cdot)$ of the channel, and the Kronecker delta, δ. Assuming Jake's Doppler spectrum we have e.g. $\Theta(\lambda) = \mathrm{J}_0(2\pi f_{\mathrm{D,max}} T_s \lambda/N)$, where the 1st kind Bessel function is denoted by $\mathrm{J}_0(\cdot)$, the maximum Doppler frequency by $f_{\mathrm{D,max}}$, and the OFDM-symbol duration by T_s. The modulo function is denoted by $(\cdot)_N$.

A. Simplified Timing Metric

Eq. (10) is optimal in finding the timing and frequency offset parameters in the sense that all available information is utilized, i.e., all receive signals, correlations and the signal-to-noise power ratio (SNR). Unfortunately, this makes it impractical, since this knowledge is not always at hand. Subsequently we introduce certain simplifications which render the metric suboptimal, yet still efficient. These simplifications involve a summation over a finite number of OFDM symbols, neglecting correlations, neglecting SNR, and a two stage approach for firstly finding the timing offset and secondly the frequency offset.

A practical version of the timing metric (10) emerges if we truncate the sum to include only the recent $B+1$ OFDM-symbols, i.e., a finite number of OFDM-symbols

$$\lambda_1(\theta_i,\varepsilon_i) = \sum_{i'=i-B}^{i} \log p(\boldsymbol{z}(i')|\theta_i,\varepsilon_i)\,. \qquad (14)$$

Note that unlike (10) the left hand side of (14) is now dependend on the OFDM-symbol index i, i.e., it is regularly updated.

Furthermore, we assume spatially uncorrelated and temporally fully correlated antenna signals as well as a low noise scenario, which is clearly suboptimal. However, this yields a robust and easily implementable estimator. With the negative Euclidean distance, $\Lambda(k) = -\parallel \boldsymbol{y}(k) - \boldsymbol{y}(k+N) \parallel^2$, between all antenna signals in the k-th time instant, we have

$$\lambda_2(\theta_i) = \sum_{i'=i-B}^{i} \sum_{k'=-N_s}^{-1} \Lambda(k'+\theta_i+i'Z)\,. \qquad (15)$$

Unfortunately, the inner summation over N_s for $N_s < N_{\mathrm{g}}$ does not lead to a unique peak in the timing metric. Instead a plateau is established, which increases the variance of the detected timing offset [6]. Our simulation results indicate that simple rectangular filtering concentrates the timing plateau in a triangular shape whose peak is a robust timing offset indicator. The width of the rectangular filter is chosen to cover the timing plateau as if only AWGN were present, i.e., $N_{\mathrm{g}} - N_s + 1$.

$$\lambda_3(\theta_i) = \sum_{i'=i-B}^{i} \sum_{k'=-N_s}^{-1} \sum_{k''=N_{\mathrm{g}}-N_s}^{0} \Lambda(k'+k''+\theta_i+i'Z) \qquad (16)$$

Having determined the timing offset by means of (16), i.e., $\hat{\theta}_i = \mathrm{argmax}_{\theta_i}\,\lambda_3(\theta_i)$, we find an estimate of the frequency offset by

$$\hat{\varepsilon}_i = -\sum_{i'=i-B}^{i} \sum_{k'=-N_s}^{-1} \sum_{a=0}^{N_r-1} \frac{\arg\{y_a(m)y_a^*(m+N)\}}{2\pi(B+1)N_sN_r} \qquad (17)$$

with $m = \hat{\theta}_i + k' + i'Z$.

IV. Simulation Results

A. Variance of the detected timing offset

We begin the assessment of our synchronisation scheme by examining the variance of the detected timing offset $\hat{\theta}$ against the true value vs. E_{b}/N_0. Fig. 2 depicts results for a statistical WSSUS channel with uniform power delay profile of length $L = 10$ and Jakes' Doppler spectrum with $f_{\mathrm{D,max}}T_s = 0.05,\ 0.15$. One receive antenna, $N_r = 1$, is assumed. The number of subcarriers and the length of the cyclic prefix are $N = 64$ and $N_{\mathrm{g}} = 16$. A convolutional code is used with code rate $1/2$.

The size of the inner correlation window is varied from $N_s = 1$, for which only one pair of symbols in the CP and the core symbols is correlated, over $N_s = 6$, for which all of the ISI-free portion of the CP is used for correlation, to $N_s = 14$, for which the correlation is extended over the ISI-contaminated parts of the CP. The number of OFDM-symbols, B, is also varied, i.e., $B = 0, 1, 64$.

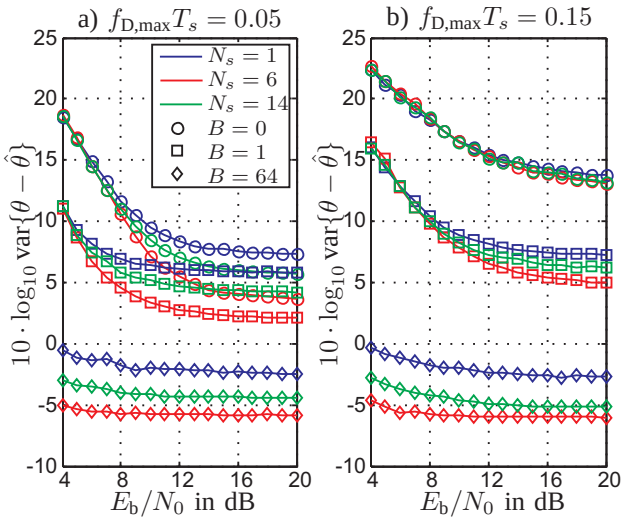

Fig. 2. Variance of detected timing offset for moderate and fast fading, $N_r = 1$, $L = 10$, correlation and SNR are perfectly known, $\varepsilon = 0$

Let us consider the influence of the number of exploited OFDM-symbols. If $B = 0$, i.e., the timing offset is determined based on one OFDM-symbol, the timing offset variance at $E_{\mathrm{b}}/N_0 = 4$ dB exceeds 20 dB. Including one additional OFDM-symbol, i.e., $B = 1$ decreases the variance by approx. 5 dB. Finally, using $B = 64$ additional OFDM-Symbols serves for decreasing the variance of the detected timing offset under 0 dB.

The variance is also decreased if the inner correlation is increased from $N_s = 1$ to $N_s = 6$, such that all of the ISI-free part of the CP is utilized. In connection with $B = 64$ additional OFDM-symbols these parameters serve for a

reliable detection of the timing offset for the moderate as well as for the fast fading case.

For the case for which the inner correlation is extended over the ISI-contamined area of the CP, i.e., $N_s = 14$, we recognize a degradation of the variance. However, it still proves to be a reliable indicator of the timing offset, which is fortunate since the length of the power delay profile in practice is not always known.

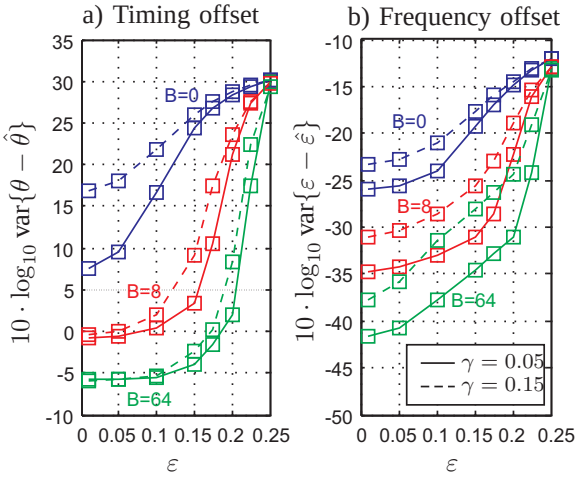

Fig. 3. Variance of timing and frequency offset estimates vs. normalized frequency offset ε for different SNRs and Doppler frequencies, length of CIR $L = 10$, size of inner correlation $N_s = 6$, $N_r = 1$

In Fig. 3 a frequency offset is present. The maximal frequency offset which can be estimated based on the cyclic prefix method (17) is 0.5 otherwise phase ambiguities occur [3]. However, since the frequency offset estimation follows upon estimating the timing estimate this maximal range is decreased. This is due to the timing offset estimator disregarding the presence of a frequency offset. Thus it is impaired, leading subsequently to a degradation of the frequency offset estimate. However, utilizing several OFDM-Symbols ($B > 0$) can alleviate this problem. Compare in Fig. 3a for a frequency offset $\varepsilon = 0.15$ the two cases $B = 0$ and $B = 64$. Based on one OFDM-symbol, i.e., $B = 0$, the variance of the timing offset is approx. 25 dB, whereas the addtional use of $B = 64$ OFDM-symbols keeps it as low as approx. -3 dB.

B. Spatial Interpolation

We now examine the performance of our synchronisation scheme in connection with the SI technique. We apply the original scheme [1] which is based on differential modulation in time direction. That same scheme is applied e.g. in DAB, where large delay spreads are expected such that the channel exhibits strong frequency selectivity. However, differential modulation will degrade if the channel is additionally characterized by fast fading. Spatial interpolation is able to alleviate this problem by transforming the time-varying channel into a time-invariant channel.

Fig. 4 shows that traditional differential modulation can not overcome the strong time-selective channel conditions. The phase variations of the rapidly fading channel

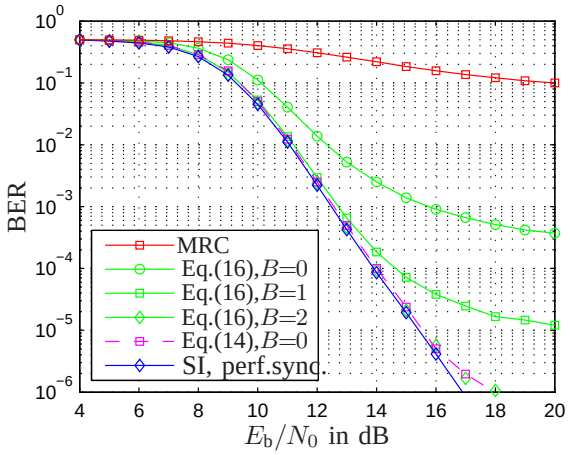

Fig. 4. Spatial interpolation for $N_r = 2$, WSSUS, $L = 10$, $N_s = 6$, $f_{\mathrm{D,max}} T_s = 0.15$, differential QPSK, $N = 64$, $N = 16$, $D = 64$

are decorrelating the subcarriers in consecutive OFDM-symbols. Hence, differential demodulation fails to recover the transmitted data symbols. Applying SI with $N_r = 2$ antennas on the other hand successfully avoids any error-floor.

Let us consider the influence of timing synchronisation. If synchronisation is based on (14) the correlation as well as the SNR are perfectly known to the receiver. Then one OFDM-symbol is already sufficient to achieve reliable timing synchronisation. If the synchronisation is based on (16) the correlation and SNR are completely disregarded. Instead uncorrelated antenna signals are assumed. If this scheme makes use of only one OFDM-symbol an error-floor of $4 \cdot 10^{-4}$ is established, which is successfully decreased by additional OFDM symbols ($B > 0$).

C. Raytracing Channel Model, Antenna Characteristics

Spatial interpolation relies on receiver-side knowledge about the channel correlations, which is used to render the channel time-invariant. For the results in Fig. 4 these correlations were perfectly known. Additionally we assumed that the ULA-antennas receive the transmitted signal via ideally delayed channel impulse realizations without mutual coupling of the single antennas. To verify the effectiveness of the SI technique for the case when these conditions are violated, we conducted ray-tracing simulations.

To generate realistic channel impulse responses (CIRs) a 3D ray-tracing propagation model and a track environment typical for high-speed trains has been used. The environment consists of a concrete ground floor and noise barriers as well as metallic tracks and pairs of pylons. A high-speed train moves along the track with 400 km/h. The movement is implemented by the train taking sequential positions within the scenario. In order to have a comprehensive description of the channel the distance between two train positions is 1 mm which is equal to 9 μs in time. On top in the middle of the train the mobile antenna is placed. Three base stations with omnidirectional antennas are positioned every 500 m along the track. They work in a common frequency mode,

i.e. all of them send the same synchronized signal. A more detailed description of the simulated scenario is given in [7].

The wave propagation is modeled by a ray-tracing tool. This takes into account multiple reflection, multiple diffraction as well as scattering [8]. The simulation frequency is 24.125 GHz which is situated in an ISM (industrial, scientific and medical) band.

For the CIR calculation a special antenna arrangement is considered. Four quarter-wavelength monopoles with uniform spacing of s $= 1.8$ mm are placed in a linear constellation on top of the train. The alignment is oriented along the train track. Using a commercial code [9] the pattern of each quarter-wavelength monopole on a metallic ground plane is determined with the remaining three antennas terminated by $50\ \Omega$ impedances. These antenna patterns include the coupling losses and are completely considered in the CIR calculation. The results are compared to the CIRs for a single quarter-wavelength monopole.

The simulation parameters were chosen as follows. The sampling frequency is set to 64 MHz, the number of subcarriers to 1024, the length of the cyclic prefix to 256. The ULA mounted on top of the train consists of $N_r = 4$ mutually coupled antennas. The train is positioned in the middle between two basestations. A 10 m segment is simulated.

In Fig. 5 we have depicted the BER performance for the channel model simulated by ray-tracing. The ray-tracing data does not necessarily obey the isotropic scattering assumption of the WSSUS channel model. If the train moves in the middle of two base stations, one can expect that the maximal and minimal Doppler frequencies are dominating the correlation. These lead to a cosine shaped autocorrelation function. On the other hand if the train is close to a base station the isotropic environment is better approximated since there are dominating angles of incidence from three sides. Here one can expect a Bessel autocorrelation function.

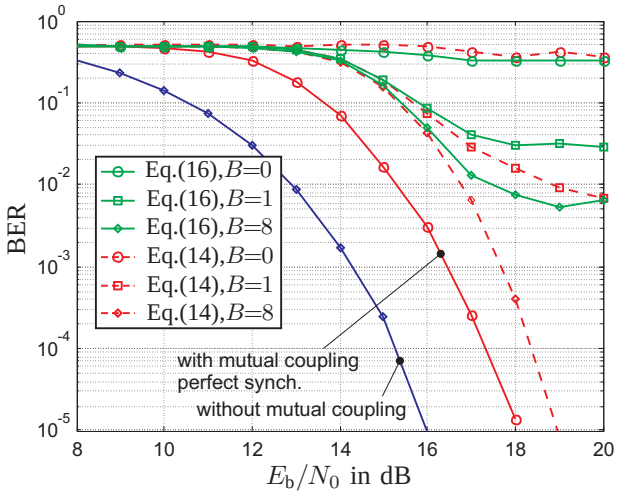

Fig. 5. BER vs. E_b/N_0 for realistic ray-tracing channel model, synchronisation based on (16), i.e., without correlation, and based on (14), i.e., with correlation and SNR, $N_r = 4$

Fig. 5 shows the performance for realistic channel data with mutual antenna coupling. As a reference we included a BER curve, which is based on the channel impulse response for a monopole antenna, which serves to set up a ULA by ideally delaying its impulse response. It is apparent from Fig. 5 that mutual coupling degrades the BER performance by approximately 2 dB. This loss is caused by the mutual coupling which violates the assumed ideal delay of the impulse responses. To determine the Wiener coefficients in (7) we prescribed specific correlations. Namely we chose a cosine function with $f_{\mathrm{D,max}}T_s = 0.14$ for the non-coupled, perfectly synchronized antennas, whereas the synchronization SI scheme with mutual coupling was simulated assuming a Bessel function with $f_{\mathrm{D,max}}T_s = 0.05$. The latter results indicates that the SI scheme in practice requires an estimation and tracking of the channel correlations, which is outside the scope of this paper and a topic of future work.

V. Conclusions

We have presented a novel timing and frequency synchronisation scheme for OFDM with spatial interpolation assuming continuous mode transmission. Our scheme is CP-based and, thus, introduces no additional training overhead. Based on a maximum-likelihood criterion, we derived suboptimal, yet still efficient timing and frequency offset estimators, which are exploiting several OFDM symbols instead of only one. This synchronisation scheme preserves the SI's ability to reduce the effective Doppler spread. Realistic channel data was generated to validate the spatial interpolation technique. We found that mutual antenna coupling introduces an SNR-loss. However, Doppler compensation is still possible. It remains a topic of future work to compensate for this mutual coupling. Simulations based on realistic channel data indicate that SI needs a reliable estimate of the channel correlations.

References

[1] H. Takayanagi, M. Okada, H. Yamamoto, "Novel Fast Fading Compensator for OFDM using Space Diversity with Space-Domain Interpolator", *54th VTC 2001 (Fall)*, Vol. 1, pp. 479-483

[2] P. Klenner, K.-D. Kammeyer, "Spatially Interpolated OFDM with Channel Estimation for Fast Fading Channels", *65th VTC 2007 (Spring)*

[3] J.-J. Beek, M. Sandell, P. O. Börjesson, "ML Estimation of Time and Frequency Offset in OFDM Systems", *IEEE Transactions on Signal Processing*, pp. 1800-1805, Vol. 45, No. 7, July 1997

[4] S. H. Müller-Weinfurtner, "On the Optimality of Metrics for Coarse Frame Synchronization in OFDM: A Comparison", pp. 533-537, PIMRC 1998, Boston USA

[5] B. Ai, Z. Yang, J. Ge, Y. Wang, Z. Lu, "On the Synchronization Techniques for Wireless OFDM Systems", pp. 236-244, IEEE Trans. on Broadcasting, Vol. 52, No. 2, June 2006

[6] T. M. Schmidl, D. C. Cox, "Robust Frequency and Timing Synchronization for OFDM", pp. 1613-1621, IEEE Trans. Comm., Vol.45, No.12, Dec. 1997

[7] S. Knörzer, M.A. Baldauf, T. Fügen, W. Wiesbeck, "Doppler Spread Reduction by Application of Directive Antennas for an OFDM-MISO Train Communications System", 4th Int. Workshop on Intelligent Transportation, pp. 143-148, March 2007

[8] T. Fügen, J. Maurer, T. Kayser, W. Wiesbeck, "Capability of 3-D Ray Tracing for Defining Parameter Sets for the Specification of Future Mobile Communications Systems", IEEE Trans. on Antennas and Propagation,Vol. 54, Nr. 11, pp. 3125-3137, Nov. 2006

[9] FEKO, EM Software & Systems, http://www.feko.info